An Optimization Approach to the Design of Multi-Size Heliostat fields

E. Carrizosa[1,2], C. Domínguez-Bravo[2], E. Fernández-Cara[2,3] and M. Quero[4]

[1] Department of Statistics and Operations Research
University of Seville, Spain
ecarrizosa@us.es

[2]Institute of Mathematics of University of Seville
Spain
carmenanadb@us.es

[3] Department of Partial equations and Numerical analysis
University of Seville, Spain
cara@us.es

[4] Abengoa Solar New Technologies
Seville, Spain
manuel.quero@solar.abengoa.com

May 28, 2014

Abstract

In this paper, the problem of optimizing the heliostats field configuration of a Solar Power Tower system with heliostats of different sizes is addressed. Maximizing the efficiency of the plant, i.e., optimizing the energy generated per unit cost, leads to a difficult high dimensional optimization problem (of variable dimension) with an objective function hard to compute and non-convex constraints as well. An heuristic algorithm greedy-based is proposed to solve the problem. The numerical experiments show the advantages of combining heliostats of different sizes, in particular, if different prices apply, which is a very reasonable assumption.

Keywords: solar thermal power, multi-size heliostat field, greedy algorithm.

1 Introduction

Solar power tower (SPT) system is known as one of the most promising technologies for producing solar electricity due to the high temperatures reached that resulte in high thermodynamic performances; some reviews on solar thermal electricity technology are [1, 11, 25, 30, 31, 36]. An SPT system is here considered to consist of two elements: a tower and a field of heliostats. Direct solar radiation is reflected and concentrated by the heliostats field in a receiver placed at the top of the tower. At the receiver, the thermal energy is transferred to a heat transfer fluid to produce electricity through a conventional thermodynamic cycle. The heliostats field is considered of a group of mirrors having two-axis motion to reflect the direct light from the sun to the aim point on the receiver aperture.

The optimal design of an SPT system consists of determining the tower height, the shape and dimensions of the receiver aperture in the tower (tower optimization) and the location of the heliostats (field optimization) so as to maximize *the energy per unit cost*, see [29]. In this paper we focus only on the optimization of the multi-size heliostat field using a pattern-free method and combining two heliostat sizes.

The optimization of the field is a challenging problem due to two issues already pointed out in [16]. Firstly, the problem is of very large dimension, with hundreds (or even thousands) of variables and non-convex constraints [5]. Secondly, the objective function is nonsmooth, of black-box type and multimodal, see [8, 13, 28, 29], whose evaluation is very time consuming, mainly due to the so-called shading and blocking effects [11].

With the purpose of design the heliostats field, very frequently a geometrical pattern is imposed, i.e., the heliostats locations are assumed to follow a fixed distribution. It is commonly assumed that heliostats follow a radial-stagger pattern, as can be seen in [6, 9, 10, 23, 22, 35, 37], other distributions as spiral [26] or grid [32], are also used. These distributions are usually optimized using different parametric approaches, or used as starting solutions in a sequential optimization procedure, see [4, 6].

All the papers we are aware of assume all heliostats with identical size, this size being given as detailed for instance in [26]. Choosing all heliostats of one single size may not lead to optimal fields, as already pointed out in [15]. Moreover, the cost of an SPT system is dominated by the heliostats field as said in [17] and [20]. While there are some authors that have taken into account different heliostat geometries in order to improve the heliostats performance and cost (hexagonal [34], bubble [20], minimirror array [17], other geometries [21, 24, 38]), the design of heliostats fields using different heliostat sizes remains, as far as the authors are aware of, unexplored.

In this paper we consider two heliostat sizes, from now on called as *large-size* and *small-size*. The choice of the size of the heliostats may dramatically affect the performance of the field and also its cost. This is illustrated in Table 1 and Figure 1: the same algorithm is used to locate heliostats of small-size (points in Figure 1, left) or large-size (squares in Figure 1, right). In Table 1 we have a comparison of these fields where we find the number of heliostats (N_{hel}), the Annual Energy generated (E), the Cost of the heliostats (Ψ), when both sizes have the same price, and the ratio Annual Energy/ Total Cost (F).

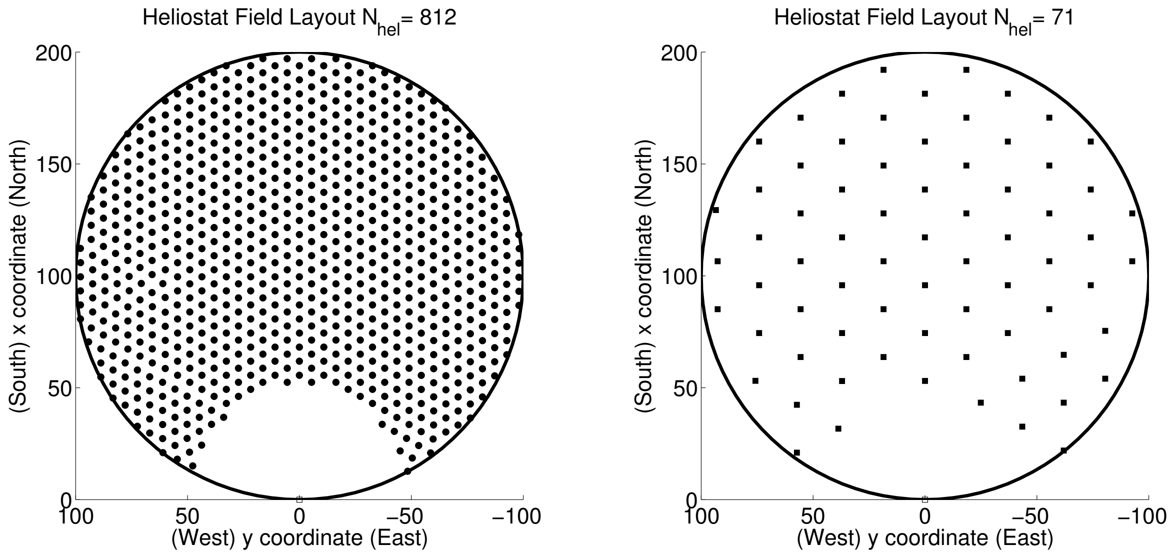

(a) Small-Size Heliostats

(b) Large-Size Heliostats

Figure 1: Circular region with heliostats of two different sizes

Size	N_{hel}	E (GWHth)	Ψ (u.c.)	F
Small	812	6.7228	0.5650	8.3213
Large	71	15.9619	1.3783	17.4656

Table 1: Field Performance

In this paper we address multi-size heliostats fields, i.e. heliostat fields with different heliostat sizes. The rest of the paper is organized as follows. In Section 2, we describe the main ingredients affecting the behavior and performance of the SPT system. Our methodology to solve the problem is explained in Section 3. In Section 4, we apply the optimization algorithm and analysis tools to a typical plant design and finally, in Section 5, our main results are summarized and some perspectives for further work are presented.

2 Problem statement

In this Section, the SPT system considered in the paper is described. We explain the meaning of the variables involved in the optimization process and the constraints that have to be satisfied. The cost and energy functions, that are the two elements to be considered in the objective function, and the optimization problem we are going to address are also described.

2.1 Decision variables

For simplicity, we assume that the tower and receiver dimensions are given, see Section 5 for some remarks on how to address the full (tower and field) optimization problem.

The heliostats locations, given by the coordinates (x, y) of their centers, and the heliostat sizes d, are the variables to be used. All heliostats are assumed to be rectangular, although they can have different dimensions. We assume that the set $\mathcal{D}$ of all the possible heliostats dimensions is finite and given.

From now on we will denote by Ω the collections of coordinates of the centers and sizes of the heliostats, namely (x, y, d). We denote by $|\Omega|$ the cardinality of Ω i.e., the total number of heliostats. The set Ω is described as follows, where N_{hel} denotes the total amount of heliostats in the field, $\mathcal{S}$ denotes the set of heliostats coordinates and $\mathcal{D}$ the set of heliostat sizes:

$$\Omega = \left\{(x^i, y^i, d^i) \text{ for } i \in [1, N_{\text{hel}}] \text{ with } (x^i, y^i) \in \mathcal{S} \text{ and } d^i \in \mathcal{D}\right\} .$$

2.2 Constraints

The annual energy function, defined below, is calculated through an annual and daily integration process. We will denote by $\Pi_T(\Omega)$ the power input at time T for a given SPT configuration. Usually, when designing a SPT plant, a fixed time is used to evaluate the plant operation. This time is known in the literature as the *design point* denoted by T_{d}. Let $\Pi_{T_{\text{d}}}(\Omega)$ be the power input obtained at the design point, where a minimal power input has to be achieved, that is:

$$\Pi_{T_{\text{d}}}(\Omega) \geq \Pi_0 \,. \tag{1}$$

Due to technical reasons, the heliostats must be located within a given region $\mathcal{S}_0 \in \mathbb{R}^2$. This defines a constraint on the heliostat locations:

$$\mathcal{S} \subset \mathcal{S}_0 \,. \tag{2}$$

The heliostats located in the field have to move freely avoiding collisions with other heliostats. Consequently, we have to consider other constraints forcing the heliostats not to overlap. These constraints should depend on the heliostats size:

$$||(x^i, y^i) - (x^j, y^j)|| \geq \delta_i + \delta_j \quad \text{ for } i \neq j \,, \tag{3}$$

where $\delta_i, \delta_j > 0$ are given parameters related with the heliostats size d^i and d^j respectively.

2.3 Functions

The cost and annual energy are the functions involved in the optimization problem. The cost function C takes into account the investment in power plant equipment (tower, receiver and heliostats), purchasing of land and civil engineering costs:

$$C(\Omega) = K + \Psi(\Omega), \text{ with } \Psi(\Omega) = \sum_{d \in \mathcal{D}} c_d \left| \left\{ i \in [1, N_{\text{hel}}] : d^i = d \right\} \right| , \tag{4}$$

where K is a constant including all fixed costs and c_d are positive constants representing the price of each heliostat of size $d \in \mathcal{D}$.

The annual energy input function E takes the form:

$$E(\Omega) = \int_O^T \tilde{\Pi}_t(\Omega)\, dt\,, \tag{5}$$

where $\tilde{\Pi}_t$ denotes the polinomial fitting of the power input reached by the system at each time instant t.

The power input values of the system are calculated by adding the power values reached by each heliostat located in the field, detailed as follows:

$$\Pi_t(\Omega) = I(t)\eta(t) f_{ref} \sum_{i=1}^{N_{\text{hel}}} \varphi(t, x^i, y^i, d^i, \Omega)\,. \tag{6}$$

Here $I(t)$ is the so-called instantaneous direct solar radiation, $\eta(t)$ is a mesure of the radiation losses, f_{ref} is the heliostat reflectance factor and φ represents the product of the efficiency factors (usual in this framework), that is, $\varphi = f_{at}\, f_{cos}\, f_{sb}\, f_{sp}$.

In particular, $f_{at} = f_{at}(x, y)$ is the atmospheric efficiency, [2, 13]; $f_{cos} = f_{cos}(t, x, y)$ is the cosine efficiency, [13]; $f_{sb} = f_{sb}(t, x, y, d, \Omega)$ is the shadowing and blocking efficiency [10, 33, 36], and, finally, $f_{sp} = f_{sp}(t, x, y, d)$ is the interception efficiency or spillage factor [12, 19, 18].

We do not give here a deep detail of the model used to compute the annual energy of the plant. We use the NSPOC procedure, which is described in [14] and we refer the reader to [2, 12, 13, 36] for further details.

2.4 Optimization Problem

In this problem the number of heliostats is not fixed in advance. Even fixing the number of heliostats, the huge number of variables, around 3,000 in recent commercial plants [7], and the high computation time needed to evaluate the energy function, due to the shadow and blocking effects, make this problem very difficult to solve as pointed out in [11].

The optimization problem we are addressing can be written as follows, when the energy generated per unit cost is considered as objective function:

$$(\mathcal{P}) \left\{ \begin{array}{ll} \max\limits_{\Omega} & F(\Omega) = E(\Omega)/C(\Omega) \\ \text{subject to} & \Pi_{T_\text{d}}(\Omega) \geq \Pi_0 \\ & \Omega \subset \mathcal{S}_0 \times \mathcal{D} \\ & ||(x^i, y^i) - (x^j, y^j)|| \geq \delta_i + \delta_j \\ & \text{ for } i \neq j\,. \end{array} \right.$$

The heliostat efficiencies are dependant on the heliostat surface and its position in the field, as can be appreciate in (6). Hence the heliostats performance is different depending on their size. Our goal is to solve problem $(\mathcal{P})$, that is to design a multi-size field of heliostats trying to maximize the annual energy generated per unit cost.

3 Field optimization

Our goal is to solve problem $(\mathcal{P})$, that is to design a field of heliostats when different heliostat sizes are involved as optimization variables. We are going to describe in this Section the algorithm that we present to solve the problem.

The heuristic algorithm presented in this paper, is called the *Expansion-Contraction Algorithm*. As initial step the algorithm generates a large-size heliostat field following another algorithm called *Greedy Algorithm*. Then two phases, expansion and contraction, are applied into this initial field and repeated until no improvement is obtained in the objective function. At the *Expansion Phase*, the field is filled with small-size heliostats and at the *Contraction Phase* the best heliostats are selected according to their annual efficiency.

As we have already mention the algorithm presented in this paper is based on an algorithm called *Greedy Algorithm* and designed to locate heliostats when considering only one heliostat size. This algorithm have been presented in [8], where the tower and receiver are also considered as variables in the optimization process. It is a greedy-based algorithm that sequentially locates the heliostats one by one on the best feasible position in the field at each step k, that is, the location where the annual energy of the whole field is largest, until the power constraint is reached. The algorithm is briefly described in next subsection.

When different heliostat sizes are involved in the location problem the cost function become an important factor, as it is related with the heliostat size. In the *Expansion-Contraction Algorithm* different heliostat prices are taken into account for the different heliostat sizes.

As far as we are aware of, no paper addresses problem $(\mathcal{P})$, which allows heliostats to be of different sizes. Moreover, our approach is different from others in the literature for single-size heliostats in several aspects:

- There is no need of a starting configuration, i.e., no initial field is needed.
- A pattern-free strategy is used to locate heliostats (e.g. we do not assume that the field has to possess a radially staggered shape).
- The number of heliostats is selected according to the power input requirements, avoiding oversizing the whole heliostat field.

In the next subsections we are going to give a brief introduction to the *Greedy Algorithm* (see [8] for more details) and a complete explanation of the *Expansion-Contraction Algorithm*.

3.1 Greedy Algorithm

As the *Expansion-Contraction Algorithm* is based on the *Greedy Algorithm*, we are going to give a brief description of the *Greedy Algorithm* (see [8] for more details).

This algorithm is a greedy-based procedure that sequentially locates the heliostats one by one on the best feasible position in the field at each step k. As the heliostat cost is independent on the heliostat location, we can consider as objective function the annual energy function, E. The heliostats are located freely, without any pre-arranged distribution. Only two geometrical constraints, already mentioned, have to be taken into account to locate the heliostats: the field shape constraint (2) and the heliostat center constraints to avoid collisions, see (3). The annual energy is modified at each step as well as the shading and blocking effects that the new heliostat is causing in the field. Once a new heliostat is located and the shading and blocking effects are incorporated, the process is repeated.

Note that to be consistan we use the same notation (x, y, d) although in this specific case the size d is not considered as an optimization variable. Obviously, the first problem $(\mathcal{P}^1)$ involves locating the first heliostat center when only the field shape constraint is considered:

$$(\mathcal{P}^1)\begin{cases} \max\limits_{(x,y)} & E(\{(x, y, d)\}) \\ \text{subject to} & (x, y) \in \mathcal{S}_0\,. \end{cases}$$

This problem has an easy-to-handle objective function, as plotted in Figure 2(a). In return, when we have already located $k-1$ heliostats and we have obtained a field $\Omega^{k-1} = \left\{(x^1, y^1, d), \ldots, (x^{k-1}, y^{k-1}, d)\right\}$ that fulfill (2) and (3), the problem $\left(\mathcal{P}^k\right)$ described below is difficult to solve, since non-convex constraints are involved and the energy function has a complex shape due to the shadowing and blocking effects, see Figure 2(b).

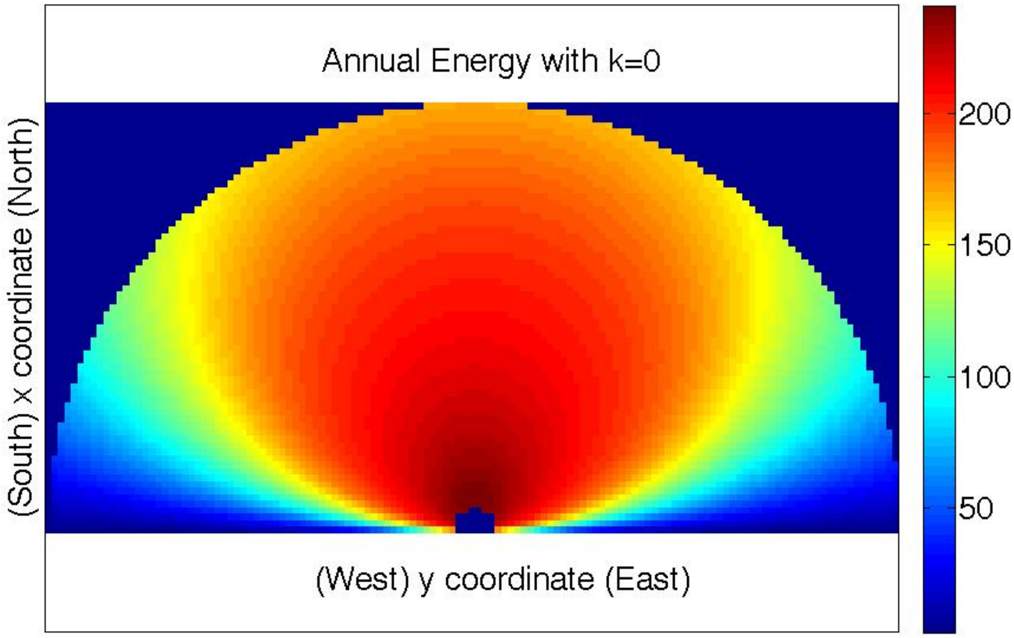

(a) Step ($k = 0$)

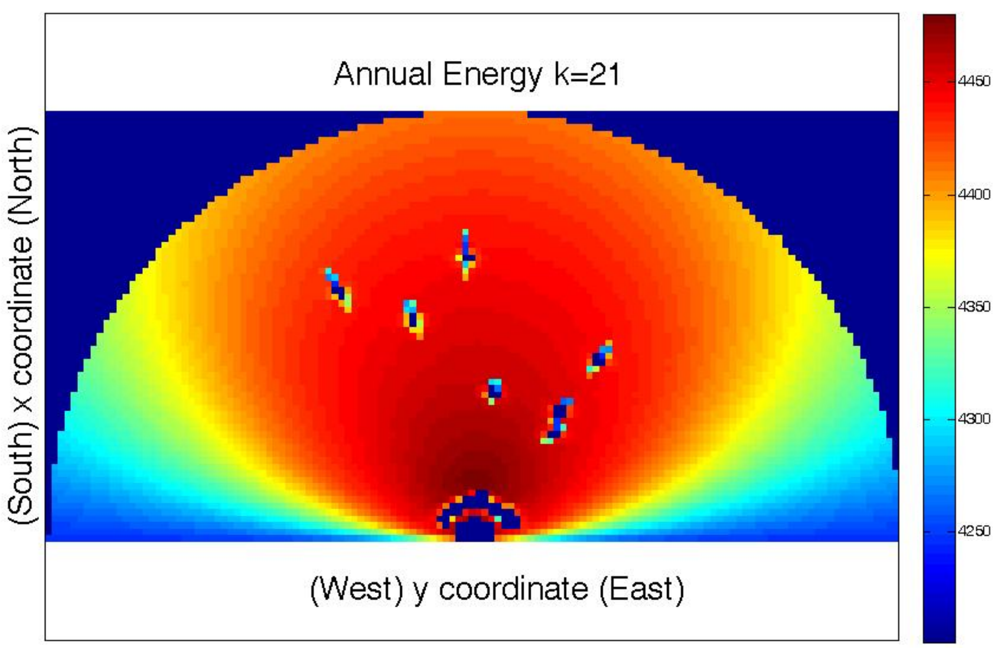

(b) Step ($k = 20$)

Figure 2: Annual Energy

Let us introduce the notation $\Omega^k = \Omega^{k-1} \cup \{(x, y, d)\}$, where (x, y) denotes the variable with respect we maximize in problem $\left(\mathcal{P}^k\right)$, since the heliostat size d is fixed for the moment. Now, we focus on the problem of finding the optimal location of a new heliostat in $\left(\mathcal{P}^k\right)$ problem:

$$\left(\mathcal{P}^k\right) \begin{cases} \max\limits_{(x,y)} & E(\Omega^{k-1} \cup \{(x, y, d)\}) \\ \text{subject to} & (x, y) \in \mathcal{S}^0 \\ & ||(x^i, y^i) - (x, y)|| \geq 2\delta \\ & \forall (x^i, y^i, d) \in \Omega^{k-1} \text{ with } 1 \leq i \leq k-1\,. \end{cases}$$

As shown in Figure 2(b), when $k > 0$ this is a multi-modal problem with non-convex constraints. A multistart procedure is used to avoid local minima. The multistart algorithm begins with N_{ini} different random feasible solutions of the fixed size. The best solution is obtained taking into account the annual energy given by each configuration.

3.2 Expansion-Contraction Algorithm

The *Expansion-Contraction Algorithm* is designed for heliostat location problems with different heliostat sizes, we are going to consider two sizes, denoted by *large-size* and *small-size* as we have already mentioned. The algorithm starts with a feasible large-size heliostats field that reaches the power input constraint (1) and then makes a series of Expansion-Contraction phases of the field using small-size heliostats. The two different phases: Expansion and Contraction, are explained below.

The *Expansion Phase* consists of oversizing the initial field using small-size heliostats until a certain power input value Π_0^+, greater than Π_0, is reached. Small-size heliostats are more versatile, they are expected to fill-in holes between large-size heliostats and to reduce spillage losses in lateral regions, reaching higher energy values.

Once the oversized mixed-field is calculated, the heliostats are arranged according to their annual energy values per unit area. The best heliostats are sequentially selected at the *Contraction Phase* and the final number of heliostats of the mixed-field is given by Constraint (1).

These procedures, oversize and selection, are well-known in these type of problems because they are used in common field design strategies with fixed pattern to determine the final amount of heliostats, [4, 10, 23, 37, 26].

The *Expansion-Contraction Algorithm* is described in Algorithm 1. As initial data the power values Π_0 and Π_0^+ are required. In the initial step the field Ω_0 reaching the power value Π_0 is designed using *Greedy Algorithm*. The field efficiency at each step $F(\Omega_k)$ is denoted by F_k, and during the process the best field obtained and its objective value are stored in Υ_{field} and Υ_{obj} respectively.

We denote by Ω_k^+, respectively Ω_k^-, the fields obtained at each Expansion, resp. Contraction, phase at step k. The algorithm continues up to the maximum number of iterations, k_{max} or when no improvement in the objective function is obtained; and returns as solution the best field obtained Υ_{field} according to its objective value Υ_{obj}.

Algorithm 1 Expansion-Contraction Algorithm

Require: Π_0 and Π_0^+

$\boxed{\Omega_0} \leftarrow \begin{cases} \text{Create initial field using Large-size heliostats with } \textit{Greedy Algorithm.} \\ \text{Stop when } \Pi_0 \text{ is reached.} \end{cases}$

$F_0 \leftarrow F(\Omega)$

$\Upsilon_{obj} \leftarrow F_0$

$\Upsilon_{field} \leftarrow \Omega_0$

$k \leftarrow 0$

while $k \leq k_{max}$ **do**

Expansion Phase:

$\boxed{\Omega_k^+} \leftarrow \begin{cases} \text{Oversize } \Omega_k \text{ using small-size heliostats with } \textit{Greedy Algorithm.} \\ \text{Stop when } \Pi_0^+ \text{ is reached.} \end{cases}$

Contraction Phase:

$\boxed{\Omega_k^-} \leftarrow \begin{cases} \text{Sort } \Omega_k^+ \text{ according to: Individual Annual Energy/ Heliostat Surface.} \\ \text{Select the best heliostats until } \Pi_0 \text{ is reached.} \end{cases}$

Update:

$k \leftarrow k + 1$

$F_k \leftarrow F(\Omega_k^-)$

$\Omega_k \leftarrow \Omega_k^-$

if $F_k \geq \Upsilon_{obj}$ **then**

$\Upsilon_{obj} \leftarrow F_k$

$\Upsilon_{field} \leftarrow \Omega_k$

end if

end while

return $\boxed{\Upsilon_{field}}$

Note that at the *Contraction Phase*, the heliostats are sorted according to their "Individual Annual Energy/ Heliostat Surface" value. As we have already mention, in the next section we are going to study some results varying the heliostat price. We use the heliostat surface as a factor to compare the heliostats instead of the cost function as it is independent of the heliostat price selected.

This phase follows a sequential procedure because once an heliostat is deleted of the already sorted list, the values associated with the remaining ones have to be recalculated and sorted again because the deleted heliostat modifies the blocking and shadowing effects of its neighbors. This process can be done selecting carefully the active neighbors in order to avoid calculating the annual energy of the hole field and extending the computational time.

4 Results

The *Expansion-Contraction Algorithm* described in Section 3.2 has been implemented in Matlab©, using the `fmincon` routine to solve the involved local optimization subproblems. As we have already mention, we work with only two different heliostat sizes, called *small-size* and *large-size*. Large-size heliostats are the usual heliostats used in the literature ($120.3380\,m^2$ called Sanlucar120), much bigger than small-size heliostats ($4.3495\,m^2$). The specific values for each heliostat size and the optimization parameters used are shown in Table 2.

Parameter	*Default value*	*Reference*
Location and Time		
Emplacement	Sanlúcar la Mayor (Seville)	[27]
Latitude	$37^o26'$ N	[26]
Longitude	$6^o15'$ W	[26]
Design Point $T_{\rm d}$	March 21 Day 12 Hour	assumed
Design direct normal irradiation DNI	823.9 W/m^2	assumed
DNI model	cloudless skies	assumed
Tower and Receiver		
Tower optical height h	100.50 m	[26]
Aperture radius r_a	6.39 m	assumed
Aperture slope ξ	12.5	[26]
Minimum radius of the field	50 m	assumed
Receiver Technology	Saturated Steam	[27]
Thermal receiver minimal power input at $T_{\rm d}$	45.50 MWth	assumed
Large-size Heliostat		
Name	Sanlucar120	[26]
Heliostat width	12.84 m	[26]
Heliostat height	9.45 m	[26]
Heliostat optical height z_0	$5,17$ m	[27]
Heliostat minimal security distance δ	heliostat diagonal+δ_0	assumed
$\sigma_{optical}$	2.9 mrad	[26]
Small-Size Heliostat		
Heliostat width	3.21 m	assumed
Heliostat height	1.355 m	assumed
Heliostat optical height z_0	5.17 m	[27]
Heliostat minimal security distance δ	heliostat diagonal+δ_0	assumed
$\sigma_{optical}$	2.9 mrad	[26]
Field		
Slope of the field	0^o	assumed
Field shape	semicircle	assumed
Maximum size	1566869.33 m^2	assumed

Table 2: Parameter Values

The power input required at the design point Π_0 is set to 42.96 MWth. The value for the upper limit Π_0^+ is set to 54.59 MWth, corresponding to a 27% increase from Π_0.

When trying to achieve the same power input, the number of heliostats depends on the heliostat size used. The number of small-size heliostats needed to achieve the same power input at the design point than a large-size heliostats field is excessive, as can be see in the next example. A field consisting of 624 large-size heliostats achieves a power input of 45.53 MWth at T_{d} while a field consisting of 4700 small-size heliostats occupying the same surface achieves a power input of 12.70 MWth at T_{d}. Therefore, the small-size heliostats field is not sufficient to achieve the same power input at T_{d} as a large-size heliostats field when occupying the same surface.

The results obtained using the *Expansion-Contraction Algorithm* are shown in Table 3. Multi-size fields with better efficiency values than the initial single-size heliostats field are presented. The **GPS10** heliostats field, obtained using the algorithm described in article [8], is used as starting point of the Algorithm 1. Any heliostats field could be used in its place, multi-size or single-size field. In order to compare the results we use the reference plant **PS10** achieving Π_0, this field configuration is similar to a solar commercial plant located in Seville, see Figure 3(a).

As we mention in Section 2, we denote by F the energy per unit cost. In order to represent the reduction in heliostat price according to their size, we denote by F_1, respectively F_2, the energy per unit cost when considering a reduction of 20%, resp. 40%, on the small-size heliostat price. Small-size heliostats are expected to have a cheaper price than large-size heliostat because of its smaller surface, the price associated with their structural support, pedestal and foundation will be smaller see [20] and [3].

Field	N_{hel}	small-size	Large-size	$\Pi_{T_{\mathrm{d}}}(\Omega)$ (MWth)	$E(\Omega)$ (GWHth)	$F(\Omega)$	$F_1(\Omega)$	$F_2(\Omega)$
PS10	592	0	592	42.9619	121.5665	54.4701	54.4701	54.4701
Ω_1	2680	2167	513	42.9346	120.8271	54.2190	55.1923	56.2012
Ω_2	3574	3094	480	42.9688	121.1273	54.3391	55.7445	57.2218
Ω_3	3886	3418	468	42.9533	121.0970	54.3498	55.9055	57.5528
Ω_4	4018	3555	463	42.9451	121.1211	54.3655	55.9864	57.7069
Ω_5	4081	3620	461	42.9576	121.2041	54.3833	56.0351	57.7877

Table 3: Results

The Reference Field and the initial field used are shown in Figure 3. In Figure 4 the expansion and contraction process of Ω_0 are detailed. The heliostats marked in red are the heliostats sequentially selected to be eliminated due to their low “Individual Annual Energy/ Heliostat Surface” values. The evolution of this algorithm is presented in Figure 5, where the different fields obtained during the process are shown.

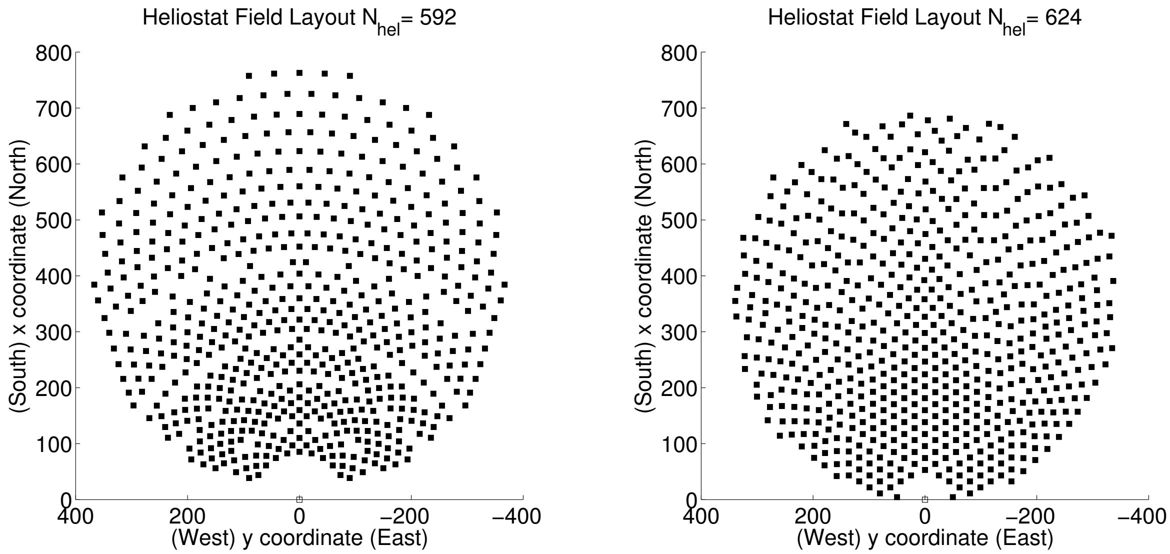

(a) **PS10** (b) Ω_0 =**GPS10**

Figure 3: The reference Field and the Initial Field

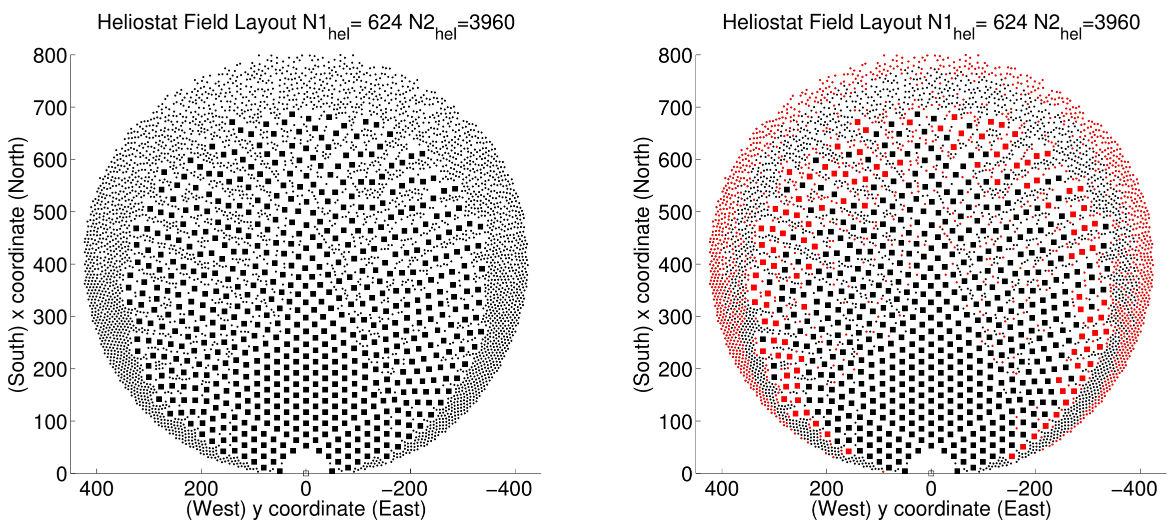

(a) Ω_0^+ (b) Ω_0^+ Selection

Figure 4: Detail of *Expansion-Contraction* Phase

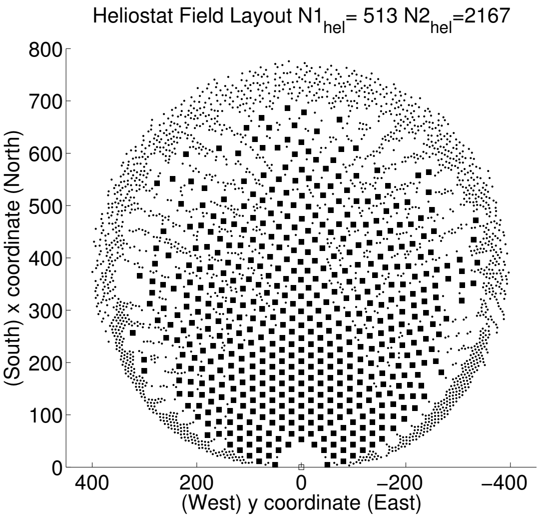

(a) Ω_1

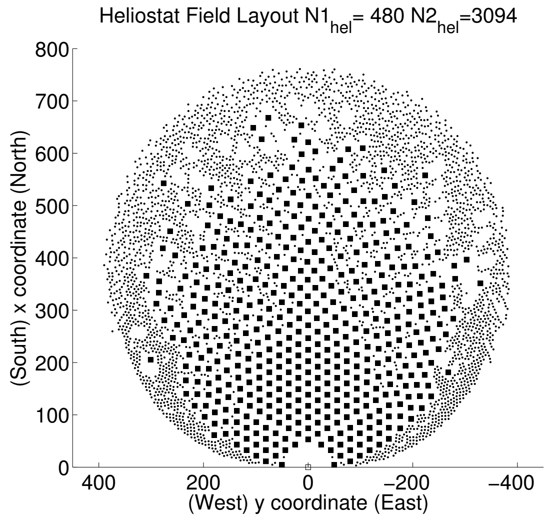

(b) Ω_2

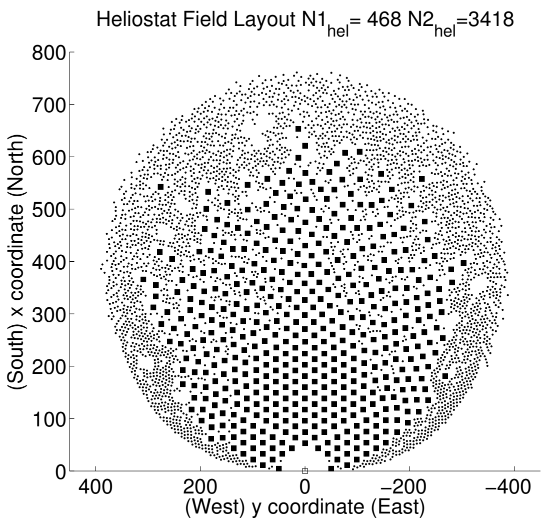

(c) Ω_3

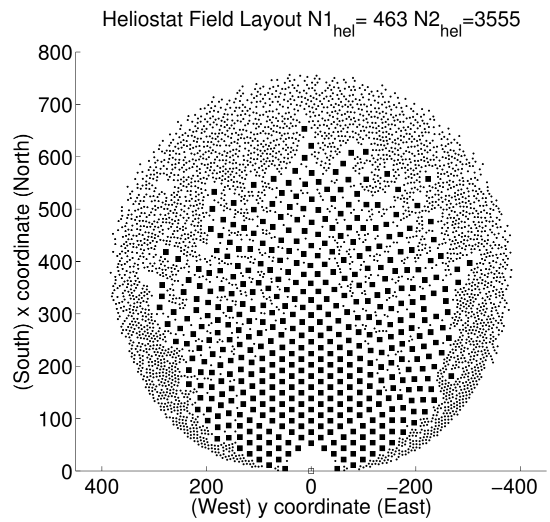

(d) Ω_4

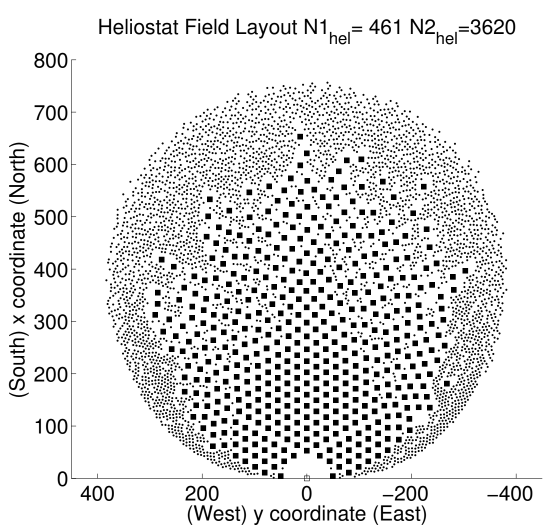

(e) Ω_5

Figure 5: Expansion-Contraction Algorithm Results (1)

The algorithm is stopped because of time limitations at Ω_5, yielding an improvement on the field efficiency of 2.87% when applied a reduction of 20% on the small-size heliostat price, and an improvement of 6.09% with a reduction of 40%.

Multi-size fields with better efficiency values than the initial single-size heliostats field are obtained. These numerical experiments show the advantages of combining heliostats of different sizes, in particular, if different prices apply, which is a very reasonable assumption.

5 Concluding remarks and extensions

An algorithm for optimizing an SPT heliostats field has been proposed, in which both the location and the size of the heliostats are simultaneously considered. The advantages of using Multi-Size heliostats fields are numerically illustrated. The Algorithm proposed tends to locate large-size heliostats in the most efficient regions of the field, and small-size heliostats, which are more versatile, in the borders and fill-in the holes.

Using the *Expansion-Contraction Algorithm* multi-sized heliostats fields are obtained with better annual energy values per unit cost that single size heliostats field, showing the usefulness of multi-sized fields.

The algorithm has been applied with two different heliostat sizes in order to show the feasibility of multi-size fields. Following the idea of the procedure presented in this paper, heliostat fields with two or more heliostat sizes can be generated.

In practice not only the heliostats field, but also the tower must be designed. This can be done following an alternating algorithm, as suggested in our paper [8]: one sequentially optimizes the field layout for a given tower design and, then, the tower design is optimized for the previously obtained field layout.

Finally, the pattern-free strategy used in this paper can be extended to cover many other situations:

- Ground irregularities in the field.
- The effect of tower shading.
- Variable (stochastic) meteorological data.
- Multiple Receivers and/or Multi-Tower plants.
- Other related factors.

6 Acknowledgements

This research has been mainly supported by Abengoa Solar N.T. and Institute of Mathematics of University of Seville (IMUS), through the research contract "CapTorSol". The authors would also like to acknowledge the support from the Government of Spain

(Grants MTM2010-15992, MTM2012-36136), Andalucía (Grant P11-FQM-7603) and EU COST Action TD1207.

References

[1] O. Behar, A. Khellaf, and K. Mohammedi. A review of studies on central receiver solar thermal power plants. *Renewable and Sustainable Energy Reviews*, 23:12–39, 2013.

[2] F. Biggs and C.N. Vittitoe. The HELIOS model for the optical behavior of reflecting solar concentrators. Technical Report SAND76–0347, Sandia National Labs., 1976. URL: `http://prod.sandia.gov/techlib/access-control.cgi/1976/760347.pdf`.

[3] J. B. Blackmon. Parametric determination of heliostat minimum cost per unit area. *Solar Energy*, 97:342–349, 2013.

[4] R. Buck. Heliostat field layout improvement by nonrestricted refinement. *Journal of Solar Energy Engineering*, 136:1–6, 2014.

[5] R. Buck, C. Barth, M. Eck, and W. Steinmann. Dual receiver concept for solar tower. *Solar Energy*, 80:1249–1254, 2006.

[6] R. Buck, A. Pfahl, and T. H. Roos. Target aligned heliostat field layout for non-linear flat terrain. In *Proceedings of the First Southern African Solar Energy Conference (SASEC 2012)*, May 2012.

[7] J. I. Burgaleta, S. Arias, and D. Ramirez. GEMASOLAR, the first tower thermosolar commercial plant with molten salt storage. In *Proceedings of SolarPACES 2011*, 2011.

[8] E. Carrizosa, C. Domínguez-Bravo, E. Fernández-Cara, and M. Quero. A global optimization approach to the design of solar power plants. Technical report, IMUS, 2013. URL: `http://www.optimization-online.org/DB\_HTML/2014/04/4305.html`.

[9] F. J. Collado. Preliminary design of surrounding heliostat fields. *Renewable Energy*, 34(5):1359–1363, 2009.

[10] F. J. Collado and J. Guallar. Campo: Generation of regular heliostat fields. *Renewable Energy*, 46:49–59, 2012.

[11] F. J. Collado and J. Guallar. A review of optimized design layouts for solar power tower plants with campo code. *Renewable and Sustainable Energy Reviews*, 20:142–154, 2013.

[12] F. J. Collado and J.A. Turégano. An analytic function for the flux density due to sunlight reflected from a heliostat. *Solar Energy*, 37:215–234, 1986.

[13] F. J. Collado and J.A. Turégano. Calculation of the annual thermal energy supplied by a defined heliostat field. *Solar Energy*, 42:149–165, 1989.

[14] L. Crespo and F. Ramos. NSPOC: A New Powerful Tool for Heliostat Field Layout and Receiver Geometry Optimizations. In *Proceedings of SolarPACES 2009*, September 2009.

[15] L. Crespo, F. Ramos, and F. Martínez. Questions and answers on solar central receiver plant design by NSPOC. In *Proceedings of SolarPACES 2011*, 2011.

[16] P. Garcia, A. Ferriere, and A. Bezian. Codes for solar flux calculation dedicated to central receiver system applications: A comparative review. *Solar Energy*, 82:189–197, 2008.

[17] J. Göttsche, B. Hoffschmidt, S. Schmitz, and M. Sauerborn. Solar Concentrating Systems using Small Mirror Arrays. *Solar Energy Engineering*, 132:011003–011007, 2010.

[18] M. Kiera. Abbildung der sonne auf die apertur eines sonnenkrftwerkes. Technical Report imb-BT-a20000-12, GAST project, 1980.

[19] M. Kiera. Feldoptimierung bei variationen de parameters. Technical Report imb-BT-320000-05, GAST project, 1980.

[20] J. G. Kolb, S. A. Jones, M. W. Donnelly, D. Gorman, R. Thomas, R. Davenport, and R. Lumia. Heliostat Cost reduction study. Technical Report SAND2007-3293, Sandia National Labs., 2007. URL: `http://prod.sandia.gov/techlib/access-control.cgi/2007/073293.pdf`.

[21] W. Landman. Sensitivity analysis of a curved heliostat profile. In *Proceedings of Annual Student Symposium 2012 in CRSES*, 2012.

[22] F. W. Lipps and L. L. Vant-Hull. A cellwise method for the optimization of large central receiver systems. *Solar Energy*, 20:505–516, 1978.

[23] F.W. Lipps. Theory of Cellwise Optimization for Solar Central Receiver Systems. Technical Report SAND-85-8177, Houston Univ., TX (USA). Energy Lab., 1981. URL: `http://www.osti.gov/scitech/biblio/5734792`.

[24] T. R. Mancini. Catalog of solar heliostats. Technical Report III–1/00, SolarPACES, 2000. URL: `http://www.fika.org/jb/resources/Heliostat%20Catalog.pdf`.

[25] D. R. Mills. Advances in solar thermal electricity technology. *Solar Energy*, 76:19–31, 2004.

[26] C. J. Noone, M. Torrilhon, and A. Mitsos. Heliostat field optimization: A new computationally efficient model and biomimetic layout. *Solar Energy*, 86:792–803, 2012.

[27] R. Osuna, V. Fernández, S. Romero, M. Romero, and M. Sánchez. PS10: a 11.0-MWe Solar Tower Power Plant with Satured Steam Receiver. In *Proceedings of SolarPACES 2004*, 2004. Editors: C. Ramos and J. Huacuz.

[28] J. E. Pacheco, H.E. Reilly, G. J. Kolb, and C.E. Tyner. Summary of the Solar Two Test and Evaluation Program. Technical Report SAND2000-0372C, Sandia National Labs., 2000. URL: `http://www.stratosolar.com/uploads/5/6/7/1/5671050/23_solar_2_test_and_evaluation_751185.pdf`.

[29] A. Ramos and F. Ramos. Strategies in Tower Solar Power Plant optimization. *Solar Energy*, 86:2536–2548, 2012.

[30] V. S. Reddy, S. C. Kaushik, K. R. Ranjan, and S. k. Tyagi. State-of-the-art of solar thermal power plants- A review. *Renewable and Sustainable Energy Reviews*, 27:258–273, 2013.

[31] M. Romero, R. Buck, and J. E. Pacheco. An update on Solar Central Receiver Systems, Projects and Technologies. *Solar Energy Engineering*, 124:98–109, 2002.

[32] M. Sánchez and M. Romero. Methodology for generation of heliostat field layout in central receiver systems based on yearly normalized energy surfaces. *Solar Energy*, 80(7):861–874, 2006.

[33] G. Sassi. Some notes on shadow and blockage effects. *Solar Energy*, 31(3):331–333, 1983.

[34] P. Schramek and D. R. Mills. Heliostats for maximum ground coverage. *Energy*, 29:701–713, 2004.

[35] F. M. F. Siala and M. E. Elayeb. Mathematical formulation of a graphical method for a no blocking heliostat field layout. *Renewable Energy*, 23:77–92, 2001.

[36] W. B. Stine and R. W. Harrigan. *Power From The Sun*. John Wiley and Sons, 2001. URL: `http://www.powerfromthesun.net/book.htm`.

[37] X. Wei, Z. Lu, Z. Wang, W. Yu, H. Zhang, and Z. Yao. A new method for the design of the heliostat field layout for solar tower power plant. *Renewable Energy*, 35(9):1970–1975, 2010.

[38] C. Zang, Z. Wang, H. Liu, and Y. Ruan. Experimental wind load model for heliostats. *Applied Energy*, 93:444–448, 2012.